JOURNAL OF COMPUTATIONAL PHYSICS 32, 24–38 (1979)

Remarks on the Solution of Poisson's Equation for Isolated Systems

J. W. EASTWOOD AND D. R. K. BROWNRIGG

Department of Computer Science, University of Reading, Whiteknights, Reading, Berkshire, England

Received August 9, 1977; revised January 19, 1978

A discussion of the solution by means of fast fourier transforms of the constant coefficient elliptic problem with isolated boundary conditions is presented. Concepts of filtering and sampling are used to show that the transform algorithm devised by Hockney [1] gives exact potential values in the computational box (c.f. remarks in [2]). The algorithm and performance of a three dimensional implementation of the transform algorithm is given. It is shown that interlaced meshes or mesh and submeshes may be employed to gain further computational economy.

1. INTRODUCTION

The transform method for solving Poisson's equation for isolated systems was first developed by Hockney [1]. The original implementation of the transform method for an isolated system, POT3, (loc cit.) is, as Hockney pointed out, wasteful in both computer time and storage. Our aim in this paper is to dispel certain erroneous ideas about the nature of the transform potential solver, and to show how economies in storage and computer time can be achieved without any substantial alteration of Hockney's algorithm. In addition, we shall indicate how further savings can be made by using new transform based algorithms.

We devote section 2 to a detailed discussion of the principles of the isolated potential solver method. This, we feel, is necessary because of the mistaken impression [2] that the transform method keeps unrealistic boundary conditions, but reduces their influence in the region of interest by moving the boundaries further away. Section 3 is devoted to a description of a three dimensional potential solver, POT5A developed by one of us (DRKB). There, we shall show that the estimates of necessary storage and computer time given by Maruhn *et al.* [2] are unduly pessimistic. In sections 4 and 5 we outline variations of the transform method designed to give further computational economies.

2. THE *FFT* METHOD FOR ISOLATED SYSTEMS

The elliptic problem, to solve

$$\nabla^2\phi(\mathbf{x}) = \rho(\mathbf{x}) \tag{1}$$

0021-9991/79/070024–15$02.00/0

subject to boundary conditions

$$\phi \to 0 \quad \text{as} \quad |x| \to \infty \tag{2}$$

may be transformed to the integral equation

$$\phi(\mathbf{x}) = \int G(\mathbf{x} - \mathbf{x}')\, \rho(\mathbf{x}')\, d\mathbf{x}' \tag{3}$$

where

$$\nabla^2 G = \delta(\mathbf{x}) \tag{4}$$

and

$$G \to 0 \quad \text{as} \quad |x| \to \infty$$

The Green's function, G, gives the response to a unit source term. In three dimensions, (4) gives

$$G(\mathbf{x} - \mathbf{x}') = \frac{1}{4\pi\, |\, \mathbf{x} - \mathbf{x}'\, |} \tag{5}$$

Given the Green's function, the convolution integral expression for the potential can be solved using fourier transforms:-

$$\begin{aligned} &G \supset \hat{G} \\ &\rho \supset \hat{\rho} \\ &\hat{\phi} = \hat{G}\hat{\rho} \\ &\hat{\phi} \supset \phi \end{aligned} \tag{6}$$

where the symbol $\supset$ is used to denote "transforms to". The discrete analogues to (1)–(6) are solved in essentially the same way; integrals become sums, fourier transforms become discrete fourier transforms. The only major difference between the discrete and continuous case is the x-space truncation of G to suppress aliases—in this instance aliases would manifest themselves as periodic boundary conditions.

The discrete problem may be derived directly from the continuous case by replacing $\rho(\mathbf{x})$ by samples of values defined on a regular array of mesh points. For simplicity, consider the one dimensional case. The sampled set of values of ρ may be described using the generalised function

$$\rho_1(x) = \text{III}\left(\frac{x}{H}\right) \rho(x) \tag{7}$$

where

$$\text{III}\,(x) \equiv \sum_{n=-\infty}^{\infty} \delta(x - n) \tag{8}$$

and $\delta(x)$ is the Dirac delta function. Substituting (7) into (3) gives

$$\phi_1(x) = H \sum_{p'=-\infty}^{\infty} G(x - x_{p'})\, \rho(x_{p'}) \tag{9}$$

where $x_{p'} = p'H$, p' is an integer and H is the spacing of the sampling points. Sampling values of ϕ_1 at the same points as those where values of ρ are defined gives the set of algebraic equations

$$\phi_1(x_p) = H \sum_{p'=-\infty}^{\infty} G(x_p - x_{p'})\, \rho(x_{p'}) \tag{10}$$

where $\phi_1(x_p)$ differs from $\phi(x_p)$ only if $\rho(x)$ is undersampled, i.e. if, as is usual in mesh calculations, the source term is specified as a set of values defined at mesh points then $\phi_1(x_p)$ is identical to $\phi(x_p)$ for all mesh points, p. The undersampling proviso is simply a statement that the mesh must be sufficiently fine to represent the source function so that the difference between the values of the true and mesh solutions is negligible.

In practical computations, $\{\rho(x_p) = \rho_p\}$ are non-zero only for a finite range of p, say 0 to $N_g - 1$. The length $L = N_g H$ is the length of the computational box. The problem is to find values of $\phi_1(x_p) = \phi_p$ for $p \in [0, N_g - 1]$, given values of G for $p \in [-(N_g - 1), (N_g - 1)]$ and ρ for $p \in [0, N_g - 1]$ i.e. to solve

$$\phi_1(x_p) = H \sum_{p'=0}^{N_g-1} G(x_p - x_{p'})\, \rho(x_{p'}) \tag{11}$$

for $p = 0, 1, 2 \cdots N_g - 1$.

Hockney's algorithm [1] replaces (11) by the cyclic convolution expression:-

$$\phi_2(x_p) = H \sum_{p'=0}^{2N_g-1} G_2(x_p - x_{p'})\, \rho_2(x_{p'}) \tag{12}$$

where $p = 0, 1, 2 \cdots 2N_g - 1$

$$\rho_2(x_p) = \begin{cases} \rho(x_p) & 0 \leqslant p \leqslant N_g - 1 \\ 0 & N_g \leqslant p \leqslant 2N_g - 1 \end{cases} \tag{13}$$

$$G_2(x_p) = G(x_p) \qquad -N_g \leqslant p \leqslant N_g - 1 \tag{14}$$

$$\rho_2(x_p) = \rho_2(x_p + 2L) \tag{15}$$

$$G_2(x_p) = G_2(x_p + 2L) \tag{16}$$

which gives the desired result that

$$\phi_2(x_p) = \phi_1(x_p) \qquad \text{for} \quad 0 \leqslant p \leqslant N_g - 1 \tag{17}$$

Equation (12) can be readily solved using FFT as described by Hockney [1]. Note that equation (12) gives the correct potential at mesh points within the computational box, i.e. the effects of periodicity are completely suppressed for mesh points 0 to $N_g - 1$. The same result holds in two and three dimensions.

An instructive interpretation of the algorithm is given in terms of sampling. We define the transform pair (fourier series):-

$$C(x_p) = \int_{2\pi/H} \frac{dk}{2\pi} \hat{C}(k)\, e^{ikx_p} \tag{18}$$

$$\hat{C}(k) = H \sum_{p=-\infty}^{\infty} C(x_p)\, e^{-ikx_p} \tag{19}$$

the sampling function $\amalg$ (c.f. [9, 10])

$$\amalg\left(\frac{ka}{2\pi}\right) \equiv \frac{2\pi}{a} \sum_{n=-\infty}^{\infty} \delta\left(k - \frac{n\,2\pi}{a}\right) \tag{20}$$

where

$$\amalg\left(\frac{ka}{2\pi}\right) \supset \frac{1}{a}\, \amalg_s\left(\frac{x_p}{a}\right)$$

$$= \frac{1}{H} \sum_{n=-\infty}^{\infty} \delta_{p,nN_2} \tag{21}$$

and

$$a = N_2 H \tag{22}$$

and the x-space truncation function

$$\Pi_s\left(\frac{x_p}{2b}\right) = \begin{cases} 1 & |x_p| < b \\ \frac{1}{2} & |x_p| = b \\ 0 & \text{otherwise} \end{cases} \tag{23}$$

where $b = N_1 H$; N_1 integer

$$\Pi_s\left(\frac{x_p}{2b}\right) \supset H \frac{\sin(N_1 kH)}{\tan(kH/2)} \tag{24}$$

The subscript s in equations (20)–(23) is used to remind readers that we use a series transform for discrete (grid point) values in x-space.

First, let us look at the case where G is not truncated. The convolution (10) may be transformed using (18) and (19) to give

$$\hat{\phi}_1(k) = \hat{G}(k)\hat{\rho}(k) \tag{25}$$

Sampling k space at interval (π/L) $(a = 2L)$ leads to a periodicity, period $2L$ in x-space:-

$$\text{Ш}\left(\frac{kL}{\pi}\right) \hat{\phi}_1(k) \supset H \sum_{p'} \frac{1}{a} \text{Ш}_s\left(\frac{x_{p'}}{a}\right) \phi(x_p - x_{p'})$$

i.e.

$$\text{Ш}\left(\frac{kL}{\pi}\right) \hat{\phi}_1(k) \supset \sum_{n=-\infty}^{\infty} \phi_1(x_p - 2nL) \tag{26}$$

Multiplying the x-space sum in (26) by the truncation function $\prod_s (x_p/2L)$ (and performing the corresponding convolution in k-space) reduces (26) to a form which may be solved using the FFT algorithm. However, since ϕ_1 is generally non-zero for all p, the effect is to leave the periodic boundary conditions in the problem as stated by Maruhn *et al.* [2].

When G is truncated, we obtain the algorithm devised by Hockney. The convolution sum (10) is replaced by

$$\phi_2'(x_p) = H \sum_{p'} G'(x_p - x_{p'}) \rho_2(x_{p'}) \tag{27}$$

where

$$G'(x_p) = \prod\left(\frac{x_p}{2L}\right) G(x_p) \tag{28}$$

The convolution (27) gives the potential ϕ_2' which is non-zero for only a finite range of x $(-L$ to $2L)$ or equivalently, a finite range of $p \in [-N_g, 2N_g - 1]$ and is equal to the correct potential ϕ_1 for $x \in [0, L]$, or $p \in [0, N_g - 1]$. Sampling in k-space at interval π/L, followed by filtering in x-space reduces the transform pair to a form which may be solved using the FFT algorithm. The effect in x-space is to periodically superpose images of ϕ' at interval $2L$.

Thus if

$$\phi_2'(x_p) \supset \hat{\phi}_2'(k) \tag{29}$$

according to transforms (18) and (19), then k-space sampling gives

$$\text{Ш}\left(\frac{kL}{\pi}\right) \hat{\phi}_2'(k) \supset \sum_{n=-\infty}^{\infty} \phi_2'(x_p - 2nL) = \phi_2(x_p) \tag{30}$$

Taking values in the interval $x \in [0, 2L]$, $p \in [0, 2N_g - 1]$ gives

$$\phi_2(x_p) = \sum_{n=-\infty}^{\infty} \phi_2'(x_p - 2L) = \phi_2'(x_p) = \phi_1(x_p) \qquad p \in [0, N_g - 1]$$

and

$$\phi_2(x_p) = \phi_2'(x_p) + \phi_2'[x_p - 2L] \qquad p \in [N_g, 2N_g - 1]$$

i.e. Hocney's algorithm gives correct potentials in the interval [0, L]. The truncation of G causes the effect of periodic repeats to be limited to the "padding" region [L, $2L$]. A graphic interpretation of the effect of truncating G is shown in Fig. 1.

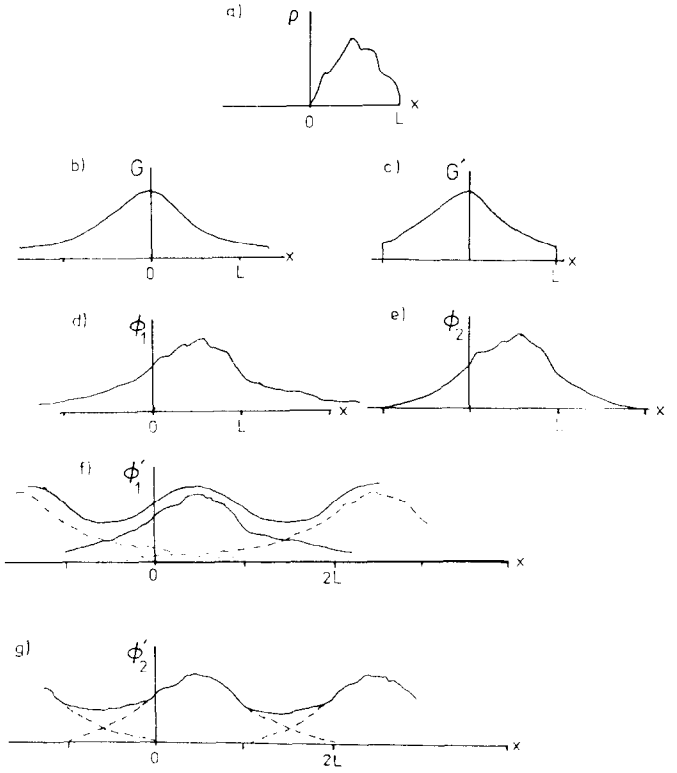

FIG. 1. A graphical interpretation of the effect of truncating the influence function, G. Solving for the potential may be regarding as convolving the set of values $\{\rho\}$ (Fig. 1a) with the influence function (Figs. 1b or 1c) to obtain potential values ϕ, and then convolving values ϕ with the sampling function $\coprod(x/2L)$ to obtain the solution ϕ'. If the influence function is truncated, then the potential ϕ_2 (Fig. 1e) is non-zero only for $-L < x \leqslant 2L$, otherwise the potential, ϕ_1, is non-zero for all x. Superposing periodic repeats of ϕ_2 gives values ϕ'_2 identical to ϕ_2 for $0 < x \leqslant L$ (Fig. 1g), whereas superposing values of ϕ_1 gives $\phi'_1 \neq \phi_1$ for all x. Thus, the effect of truncating G is to give correct potential values ($\phi'_2 = \phi_2 = G * \rho$) within the computational box ($0 < x < L$).

3. THE 3-D ISOLATED POTENTIAL SOLVER, *POT5A*

The simple minded approach to the solution of Poisson's equation in a box of $N \times N \times N$ points using the transform method would require $(2N)^3$ mesh points and approximately $5(2N)^3 \log_2(2N)^3$ real arithmetic operations. Merely by ordering the fourier analysis and synthesis correctly, storage requirements are reduced by

approximately a factor of four, and the operations count is nearly halved. These savings have been made in POT5A.

The calculation procedure in POT5A is outlined below. For simplicity, we consider the case of a cubical computational box of $N \times N \times N$ points.

Step 1. Double the length of mesh in x-direction, setting all values on the extra mesh to zero. Perform N^2 length $2N$ transforms on all lines of data parallel to the x-axis, overwriting values $\{\rho(p, q, r)\}$ by harmonics $\{\tilde{\rho}(k, q, r)\}$

Step 2. Do for all $2N$ data value planes perpendicular to the x-axis:

(a) Perform N length $2N$ transforms on lines of data parallel to y-axis.

(b) Perform $2N$ length $2N$ transforms on lines of data parallel to the z-axis.

(c) Multiply charge harmonics by influence function harmonics to obtain potential harmonics in current plane

$$\hat{\phi}(k, l, m) = \hat{G}(k, l, m)\hat{\rho}(k, l, m)$$

(d) Perform $2N$ length $2N$ inverse transforms on lines of potential harmonics parallel to z-axis.

(e) Perform N length $2N$ inverse transforms on lines of data parallel to y-axis.

Step 2 converts each plane of values $\{\tilde{\rho}(k, q, r)$; $(q, r) \in [0, N - 1]\}$ to $\{\tilde{\phi}(k, q, r)$; $(q, r) \in [0, N - 1]\}$. All other values in each plane are discarded.

Step 3. Perform N^2 length $2N$ inverse transforms on all lines of data parallel to the x-axis to obtain potential values in the computational box.

Storage required is $2N^3$ plus that needed to store influence function harmonics $\{\hat{G}\}$. If all three sides of the computational box are unequal ($NX \neq NY \neq NZ$) then

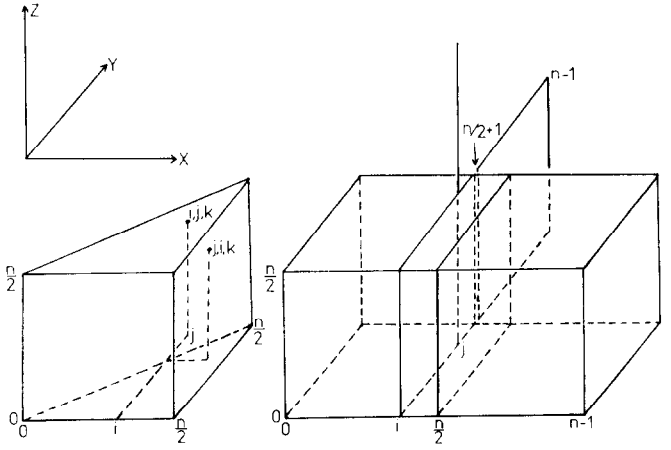

FIG. 2. Storage diagram for POT5A. ($n = 2N$).

there are $NX \times NY \times NZ$ distinct values of $\hat{G}$. Two sides equal (say $NX = NY$) introduce further symmetries reducing the number to approximately $\frac{1}{2}NX \times NY \times NZ$. The forty-eight symmetry of the cubic lattice gives a further factor of $\frac{1}{3}$ when $NX = NY = NZ$.

Fig. 2 shows the total storage region required for the calculation. The left hand triangular based region is that required for the influence function transform in the case where the number of points in x and y directions is the same as in POT5A, illustrating the reflection of values in the $x\,y$ diagonal. The left hand half of the double cube is the region where charges lie, the right hand half and the two dimensional slab of storage in the $y\,z$ plane constituting the extra storage required. The $2N$ line of sotre in the z direction corresponds to the input/output vector for the fourier analysis routine.

The arithmetic operation count for a cubic mesh of side N is as follows

Step	Number of Operations
1	$N^2(2.5 \times 2N \log_2(2N))$
2a	$2N \times N(2.5 \times (2N) \log_2(2N))$
2b	$2N \times 2N(2.5 \times (2N) \log_2(2N))$
2c	$2N \times (2N)^2$
2d	$2N \times 2N(2.5 \times (2N) \log_2(2N))$
2e	$2N \times N(2.5 \times (2N) \log_2(2N))$
3	$N^2(2.5 \times 2N \log_2(2N))$

Total: $\frac{7}{12}[5 \times (2N)^3 \log_2(2N)^3] + (2N)^3 \simeq \frac{7}{12}[5(2N)^3 \log_2(2N)^3]$

c.f. simple minded approach, where the operations count is approximately $5(2N)^3 \log_2(2N)^3$. For comparison, timings of POT5A and a triply periodic region potential solver, POT6A, are given in Table 1 for a variety of charge mesh sizes. The charge mesh dimension for POT5A is an integer power of two plus one, while that for POT6A is an integer power of two.

The calculations were performed on an IBM 370/195 using Hockney's FOUR67 FFT [3].

The factor of 7/12 improvement over the simple approach is illustrated by comparison of the timings for instance, of the 17^3 POT5A and the 32^3 POT6A, each of which use the same overall mesh. However, despite the fact that a factor of nearly two speedup is obtained by suitably ordering the operations, the method is still about four times slower than the straightforward periodic case. In the next section, a technique which allows a further speedup is discussed.

TABLE 1

POT5A		POT6A	
Charge Mesh	Time (secs)	Charge Mesh	Time (secs)
9^3	0.189	8^3	0.051
$17^2 \times 9$	0.667	$16^2 \times 8$	0.175
17^3	1.177	16^3	0.322
$33^2 \times 17$	4.245	$32^2 \times 16$	1.121
33^3	7.825	32^3	2.055

4. Interlaced Sampling in Transform Space

If, instead of sampling harmonics $\hat{\phi}_2'(k)$ at interval π/L, we sample at interval $2\pi/L$ we obtain

$$\text{Ш}\left(\frac{kL}{2\pi}\right)\hat{\phi}_2'(k) \supset \sum_{n=-\infty}^{\infty} \phi_2'(x_p - nL) \tag{33}$$

Similarly, by sampling again at interval $2\pi/L$, but this time on a mesh displaced by π/L, we find

$$\text{Ш}\left(\frac{L}{2\pi}\left(k - \frac{\pi}{L}\right)\right)\hat{\phi}_2'(k) \supset \sum_{n=-\infty}^{\infty} (-1)^n \phi_2'(x_p - nL) \tag{34}$$

The average of the two samples gives the same result as obtained earlier (equation (26)). A graphical interpretation of (33) and (34) is given in Fig. 3.

In one dimension, interlaced sampling is no more than an explicit statement of the final butterfly operation of the FFT algorithm. The equivalent in two and three dimensions would involve four and eight interlaced meshes, respectively. However, significant gains in two and three dimensions can be made by taking only two interlaced samples, where the second sample is on a mesh of points body centred with respect to the lattice of points of the first:-

The two samples in two dimensions are given by

$$\hat{S}_1 = \text{Ш}\left(\frac{k_1 L}{2\pi}, \frac{k_2 L}{2\pi}\right)\hat{\phi}_2'(k_1, k_2)$$

$$\supset \sum_{n_1=-\infty}^{\infty}\sum_{n_2=-\infty}^{\infty} \phi_2'(x_p - n_1 L, y_q - n_2 L) \tag{35}$$

and

$$\hat{S}_2 = \text{Ш}\frac{(k_1 - \frac{1}{2})\,L}{2\pi}, \frac{(k_2 - \frac{1}{2})\,L}{2\pi}\,\hat{\phi}_2'(k_1, k_2)$$
$$\supset \sum_{n_1}\sum_{n_2}(-1)^{n_1}(-1)^{n_2}\,\phi_2'(x_p - n_1L, y_q - n_2L) \tag{36}$$

Averaging the result of the two samples gives

$$\frac{(\hat{S}_1 + \hat{S}_2)}{2} \supset \sum_{n_1=-\infty}^{\infty}\sum_{n_2=-\infty}^{\infty}\phi_2'(x_p - n_1L, y_q - N_2L) \qquad [n_1 + n_2 \text{ even}] \tag{37}$$

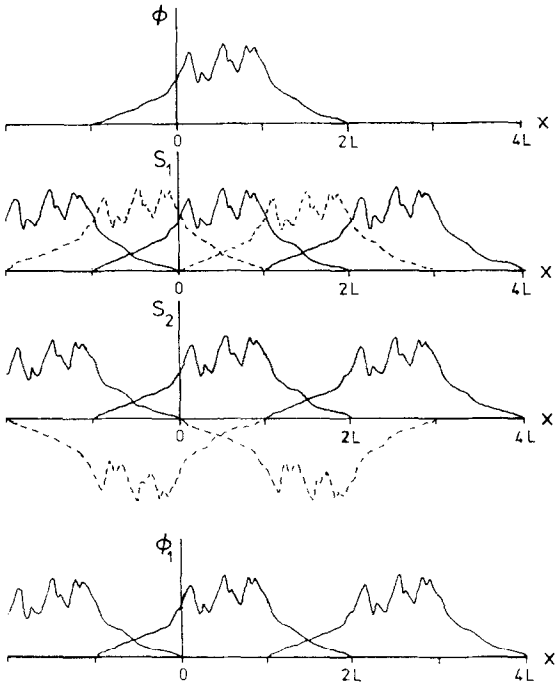

FIG. 3. A graphical interpretation of the interlaced sampling algorithm. The convolution of the source function, ρ, (non-zero in the range 0 to L) with the Greens function, G (non-zero in the range $-L$ to L) give the potential ϕ which is correct in the range 0 to L, and nonzero only in the range $-L$ to $2L$ (figure 3a). Sampling even harmonics of potential (figure 3b) gives a potential S, which is a superposition of periodic images of ϕ spaced at interval L. Sampling odd harmonics has a similar effect, except that alternate images have their signs reversed. Averaging S_1 and S_2 recovers correct potential values for $x \in [0, L]$ (figure 3d).

The result (37) shows that if $\{\rho(x_p)\}$ are non-zero only for points within the square connecting the mid-points of the side of the computational box, and if values $\{G\}$ are non-zero over a square lattice of points with sides twice that of the square in which values $\{\rho(x_p)\}$ are non-zero, then averaging two interlaced samples will give the correct potential, $\phi_1(x_p, y_q)$ within the square where $\{\rho\}$ are non-zero.

The basic form of the algorithm for finding the average of two interlaced samples, and thence the potential is given by equations (38)–(42). In these equations, the mesh spacing, is taken to be unity. Integer pairs $(p, q) \in [0, N-1]$ and $(k, l) \in [0, N-1]$ label mesh points within the computational box and harmonics, respectively.

Step 1. Find harmonics $\{\hat{\rho}\}$:-

$$\hat{\rho}(2k, 2l) = \sum_{p,q=0}^{N-1} \rho(p, q) \exp\left[-\frac{i\,2\pi}{N}(kp + lq)\right] \tag{38}$$

$$\hat{\rho}(2k+1, 2l+1) = \sum_{p,q=0}^{N-1} \rho(p, q) \exp\left[-\frac{i\pi}{N}(p + q)\right] \exp\left[-\frac{i\,2\pi}{N}(kp + lq)\right] \tag{39}$$

Step 2. Find potential harmonics

$$\hat{\phi}(2k, 2l) = \hat{G}(2k, 2l)\hat{\rho}(2k, 2l) \tag{40}$$

$$\hat{\phi}(2k+1, 2l+1) = \hat{G}(2k+1, 2l+1)\hat{\rho}(2k+1, 2l+1) \tag{41}$$

Step 3. Find potential by averaging samples

$$\phi(p, q) = \frac{1}{N^2} \sum_{k,l=0}^{N-1} \frac{1}{2}\left[\hat{\phi}(2k, 2l) + \exp\left[\frac{i\pi}{N}(p + q)\right]\hat{\phi}(2k+1, 2l+1)\right] \times \exp\left[\frac{i\,2\pi}{N}(kp + lq)\right] \tag{42}$$

In the form given by (38)–(42), the interlaced algorithm requires more storage and comparable time to that required by the straightforward algorithm. However, by manipulating the expressions for the odd harmonics, we obtain a simpler set of equations to solve. The procedure for even harmonics remains the same as above, and for odd harmonics takes the form:-

(i) find

$$\hat{A}(k, l) = \sum_{p,q=0}^{N-1} \rho(p, q) \cos\left(\frac{\pi}{N}(p + q)\right) \exp\left[-\frac{i\,2\pi}{N}(kp + lq)\right] \tag{43}$$

(ii) calculate

$$\hat{C}(k, l) = \hat{G}_+(k, l)\hat{A}(k, l) + \hat{G}_-(k, l)\hat{B}(k, l) \tag{44}$$

where

$$\hat{G}_\pm(k, l) = \hat{G}(2k+1, 2l+1) \pm \hat{G}(2k-1, 2l-1)$$

and

$$\hat{B}(k+1, l+1) + \hat{B}(k, l) = \hat{A}(k+1, l+1) - \hat{A}(k, l)$$

(iii) find

$$D(p) = \sum_{k,l=0}^{N-1} \hat{D}(k, l) \exp\left[\frac{i\,2\pi}{N}(k - l)\,p\right](-1)^l \tag{45}$$

where

$$\hat{D}(k, l) = \hat{G}_-(k, l)\hat{A}(k, l) + \hat{G}_+(k, l)\hat{B}(k, l) \tag{46}$$

(iv) find

$$C(p, q) = \frac{1}{N^2} \sum_{k,l=0}^{N-1} \hat{C}(k, l) \exp\left[\frac{i\,2\pi}{N}(kp + lq)\right] \tag{47}$$

The potential is given by

$$\phi(p, q) = \frac{1}{2N^2} \sum_{k,l=0}^{N-1} \hat{\phi}(2k, 2l) \exp\left[\frac{i\,2\pi}{N}(kp + lq)\right] + \begin{cases} \dfrac{1}{2\cos[(\pi/N)(p+q)]}\, C(p, q); & p + q \neq \dfrac{N}{2}, \dfrac{3N}{2} \\ \dfrac{i}{2N}\, D(p); & p + q = \dfrac{N}{2} \\ -\dfrac{i}{2N}\, D(p); & p + q = \dfrac{3N}{2} \end{cases} \tag{48}$$

To solve for the potential requires four periodic fourier transforms on real (or hermitian) data (equations (38), (43), (47), (48)) plus the subsidiary calculations. Correct potential values are found at $N^2/2$ points for an $N \times N$ mesh.

If we measure the calculation time of a transform on $N \times N$ real data as one unit, then the interlaced method requires $\sim$4 units to get the correct solution in a region of $N^2/2$ points. The transform method using a doubled region without ordering would require eight units for the same calculation. Careful ordering of analysis and synthesis reduces the figure to six units, approximately 50 % slower than the time estimated for the interlaced scheme.

5. Local Mesh Refinement

One advantage of the Greens function and fourier transform approach to the solution of Poissons equation is that it allows finer resolution to be added in selected areas of the computational box. The concept of spectral filtering is used in deriving mesh-submesh algorithms.

The potential calculation is split into two parts in mesh submesh algorithms: a smoothly varying part, Φ_m, and a short range rapidly varying part, Φ_s. Φ_m is

calculated using transform methods on the coarse mesh, and Φ_s is calculated either directly or by transform methods on the finer submesh.

Let $\Phi \supset \hat{\Phi}$ be the potential given by the exact calculation on a fine mesh containing both the mesh and the submesh points. In one dimension

$$\hat{\Phi}(k) = \hat{G}(k)\hat{\rho}(k) \tag{49}$$

$$= \hat{\Phi}_m(k) + \hat{\Phi}_s(k) \tag{50}$$

$$= \hat{G}\hat{S}^2\hat{\rho} + \hat{G}(1 - \hat{S}^2)\hat{\rho} \tag{51}$$

The splitting factor $\hat{S}$ may be interpreted as the transform of a finite width density profile associated with each mesh point on the composite fine mesh. $\hat{S}$ is chosen so that

(i) the short range potential term Φ_s is given by a spatially localised convolution

$$\Phi_s(x_p) = G_2 * \rho \tag{52}$$

where

$$\hat{G}_2 = \hat{G}(1 - \hat{S}^2) \tag{53}$$

and $*$ is a shorthand notation for convolution.

(ii) the smoothly varying part of the potential, $\Phi_m \supset \hat{\Phi}_m$, has a sufficiently limited spectral content to be adequately approximated by the transform method applied to the coarse mesh sample. The influence function, $\hat{G}_1$, used in the coarse mesh calculation is chosen to be the least squares fit to $\hat{G}\hat{S}^2$. The approximation ϕ_m to Φ_m is found as follows:-

(a) Filter $\{\rho(x_p)\}$ and sample every N_1^{th} point

$$f(x_p) = \text{Ш}_s\left(\frac{x_p}{N_1 H}\right)(w_1 * \rho) \tag{54}$$

thus giving modified source charges $\{f(x_p)\}$ on only the coarse mesh points

(b) solve for 'potential' on coarse mesh

$$\psi(x_p) = \text{Ш}_s\left(\frac{x_p}{N_1 H}\right)(G_1 * f) \tag{55}$$

(c) interpolate to find smoothly varying part, Φ_m, of the potential on both coarse mesh and finer submesh points

$$\phi_m(x_p) = w_2 * \psi \tag{56}$$

Steps (a) and (c) are analogous to the operations of charge assignment and potential

interpolation in particle-mesh codes. For reasons of economy, assignment and interpolation functions, w_1 and w_2, are chosen to be spatially localised.

Operations (54)–(56) give harmonics $\hat{\phi}_m(k)$:-

$$\hat{\phi}_m(k) = \hat{w}_2(k)\, \hat{g}(k) \sum_{n=0}^{N_1-1} \hat{w}_1\left(k - \frac{n\,2\pi}{N_1 H}\right) \hat{\rho}\left(k - \frac{n\,2\pi}{N_1 H}\right) \tag{57}$$

where

$$\hat{g}(k) = \sum_{n=0}^{N_1-1} \hat{G}_1\left(k - \frac{2\pi n}{N_1 H}\right) \tag{58}$$

The optimal choice of $\hat{g}$:-

$$\hat{g}(k) = \frac{\sum_{n=0}^{N_1-1} \hat{w}_1 \hat{w}_2 \hat{G}\hat{S}^2}{(\sum_{n=0}^{N_1-1} \hat{w}_1{}^2)(\sum_{n=0}^{N_1-1} \hat{w}_2{}^2)} \tag{59}$$

gives the least squares deviation, Q, of the potential of a unit source from its correct value:-

$$Q = \frac{1}{L^2} \sum_{l=0}^{N_2/2} \alpha(l, N_2/2) \left[\sum (\hat{G}\hat{S}^2)^2 - \frac{(\sum_n \hat{w}_1 \hat{w}_2 \hat{\tilde{G}}\hat{\tilde{S}}^2)^2}{(\sum_n \hat{w}_1{}^2)(\sum_n \hat{w}_2{}^2)}\right] \tag{60}$$

where L is twice the computational box length, $L = N_1 N_2 H$, and

$$\alpha(l, N_2/2) = \begin{cases} 1 & \text{if } l = 0 \text{ or } N_2/2 \\ 2 & \text{otherwise} \end{cases} \tag{61}$$

The one dimensional description of the mesh-submesh method immediately generalises to two and three dimensions. The procedure for choosing $\hat{S}$, w_1 and w_2 follows in the same manner as that used for the PPPM algorithm [7]. A more extensive analysis and practical details of the implementation of mesh-submesh algorithms will be discussed elsewhere [11].

5. Final Remarks

In this paper, we have tried to clarify two important points concerning the transform method. The first is that the transform method gives the *exact* potential rather than simply moving the periodic images further away. The second point is that storage and calculation time is *not* 2^d (d = dimension) greater than the periodic case; for example, in three dimensions, storage is only twice that required by the periodic case and calculation time is approximately four and a half times greater than for the periodic case. Further speed-up on the timings quoted can be achieved by using FFT routines written especially for short strings of real data values.

A particularly attractive feature of the transform method is the flexibility it gives in

the choice of the influence function. In large particle-mesh calculations (e.g. [4]); adjustments to $\hat{G}$ can significantly improve the quality of the representation of this dynamical system without affecting the cost of the computation (c.f. [5, 6, 7]). The flexibility is retained in the interlaced mesh variation discussed in section 4. Although the interlaced harmonics algorithm shows marginal improvement in operations count for the two dimensional case, the increased complexity of the overhead calculations in three dimensions are unlikely to show real gains over POT5A. For this reason we have not pursued it further. On the other hand, the mesh-submesh approach offers a large increase in localised spatial resolution at relatively small costs. If a seven or twenty-seven discretisation of the Laplacian operator is used on a uniform 3-D mesh, then the equivalent charge layer algorithm devised by James [8] is to be preferred to that used in POT5A because of its smaller storage requirements and calculation time. (It requires approximately half the storage and one third of the calculation time for POT5A).

ACKNOWLEDGMENT

Financial support was provided by a UKAEA extramural contract and by the S.R.C.

REFERENCES

1. R. W. HOCKNEY, *Methods Comput. Phys.* **9** (1970), 136–210.
2. J. A. MARUHN, T. A. WELTON, AND C. Y. WONG, *J. Computational Phys.* **20** (1976), 326.
3. J. P. CHRISTIANSEN AND R. W. HOCKNEY, *Comput. Phys. Commun.* **2** (1971), 127–138.
4. R. W. HOCKNEY AND D. R. K. BROWNRIGG, *Mon. Not. Roy. Astron. Soc.* **167** (1974), 351–357.
5. J. W. EASTWOOD, *J. Computational Phys.*, **18** (1975), 1–20.
6. J. W. EASTWOOD, *in* "Computational Methods in Classical and Quantum Physics" (M. B. Hooper, Ed.), pp. 196–205, Advance Publications, 1976.
7. J. W. EASTWOOD, Reference [6, pp. 206–228].
8. R. A. JAMES, *J. Computational Phys.* **25** (1977), 71.
9. R. BRACEWELL, "The Fourier Transform and Its Application," McGraw–Hill, New York, 1965.
10. E. O. BRIGHAM, "The Fast Fourier Transform," Prentice–Hall, Englewood Cliffs, N.J., 1974.
11. J. W. EASTWOOD, "The Mesh–submesh Algorithm," Reading University Computer Science Report, in preparation.